Metal/ZnO/MgO/Si/Metal Write-Once-Read-Many-Times Memory

Bosen Zhang, Cong Hu, Tianshuang Ren, Bo Wang, Jing Qi, Qing Zhang, Jian-Guo Zheng, Yan Xin, and Jianlin Liu, *Member, IEEE*

***Abstract*— Write-once-read-many-times memory (WORM) devices were fabricated using ZnO and ZnO/MgO as active layers on Si. Devices fabricated with ZnO show a different memory effect at different current compliances such as WORM at 100 μA, 500 μA, and 1 mA, resistive switching (RS) instead of WORM at 5 and 10 mA, and WORM and RS coexisting at 20, 50, and 100 mA, while devices fabricated with ZnO/MgO show WORM only at all current compliances. A few nanometers of MgO layer play a major role in preventing devices from reset at all current compliances because the much lower drift velocity of oxygen vacancy in MgO and accumulation of negatively charged O^{2-} ions at the interface between ZnO and MgO prevent the conducting filaments composed of oxygen vacancies from breaking.**

***Index Terms*— MgO, resistive random access memory (RRAM), resistive switching (RS), write-once-read-many-times memory (WORM), ZnO.**

I. Introduction

THE semiconductor technology, especially the complementary metal–oxide–semiconductor (CMOS) process, has brought sustained prosperity to the information technology over the last four decades, leading to computers with enhanced processing and storage capabilities. Memory is one of the most important parts in the semiconductor technology. As flash memory continues scaling beyond 16 nm generation, it is reaching some major physical barriers. Nonvolatile memories such as resistive-switching (RS) random access memory (RRAM) have been widely considered as alternative technologies because of the simple structure, small cell size, low power, scaling-down potential, and compatibility with the CMOS process [1]–[5]. On the other hand, as an important nonvolatile memory device which also adopts RS effect, write-once-read-many-times memory (WORM) is desirable for permanent data storage applications such as the archival storage of images and for noneditable databases where the vulnerability to breakage and the relatively high cost associated with slow and power-hungry magnetic or optical disk drives are not acceptable [6]–[9].

ZnO, an abundant and environmentally friendly oxide material, is an excellent candidate for both the RRAM and WORM applications. Reversible RS behavior suitable for random access memory was observed in monocrystalline ZnO [10], ZnO thin film [11]–[16], ZnO nanowire [17]–[19], and ZnO nanorod [20]–[23]. Compared with the research on ZnO RRAM, the effort on ZnO WORM is much smaller in scale. ZnO on Si was found to exhibit WORM characteristics, and further inclusion of a MgO thin layer between ZnO and Si led to enhanced memory performance [24], [25]. It is common to use MgO for tailoring the properties of ZnO materials and devices. For example, MgO/ZnO has been widely used as buffer layer to obtain high quality ZnO films on sapphire substrates [26], [27]. It has also been utilized in tuning the bandgap of ZnO/MgO multilayer semiconductor materials by varying ZnO layer thickness [28]. However, the reason that MgO of a few nanometers can help develop ZnO WORM on Si remains unclear. Here, we report the WORM effect of ZnO/MgO structure at a different current compliance and it is shown that the different average drift velocities of oxygen vacancy in ZnO and MgO play a major role.

II. Experiment

ZnO (70 nm), ZnO (70 nm)/MgO (2 nm), and MgO (2 nm) samples were grown on n^+-Si (100) substrates in a radio frequency (RF) plasma-assisted molecular beam epitaxy (MBE)

Manuscript received May 9, 2016; accepted July 1, 2016. Date of publication August 1, 2016; date of current version August 19, 2016. This work was supported in part by the National Natural Science Foundation of China under Grant 50902065 and Grant 11474137, in part by the Open Project through the Key Laboratory for Magnetism and Magnetic Materials, Ministry of Education, Lanzhou University under Grant LZUMMM2015012, in part by the National Science Foundation for Fostering Talents in Basic Research of the National Natural Science Foundation of China under Grant 041105 and Grant 041106, in part by the StarNet Center on Function Accelerated nano Material Engineering, in part by the Defense Microelectronics Activity under Grant H94003-10-2-1003 (3-D Electronics), in part by the Transmission Electron Microscopy through the Florida State University, and in part by the National Science Foundation within the National High Magnetic Field Laboratory, FL, USA under Grant DMR-1157490. The review of this paper was arranged by Editor U. E. Avci. *(Corresponding authors: Jing Qi and Jianlin Liu.)*

B. Zhang, C. Hu, T. Ren, B. Wang, and J. Qi are with the Key Laboratory for Magnetism and Magnetic Materials, Ministry of Education, School of Physical Science and Technology, Lanzhou University, Lanzhou 730000, China (e-mail: zhangbs14@lzu.edu.cn; huc15@lzu.edu.cn; rentsh13@lzu.edu.cn; bwang13@lzu.edu.cn; qijing@lzu.edu.cn).

Q. Zhang and J. Liu are with the Quantum Structures Laboratory, Department of Electrical Engineering, University of California at Riverside, Riverside, CA 92521 USA (e-mail: zq2000@hotmail.com; jianlin@ee.ucr.edu).

J.-G. Zheng is with the Laboratory for Electron and X-Ray Instrumentation, California Institute for Telecommunication and Information Technology, University of California at Irvine, Irvine, CA 92697 USA (e-mail: jzheng@calit2.uci.edu).

Y. Xin is with the National High Magnetic Field Laboratory, Florida State University, Tallahassee, FL 32310-3706, USA (e-mail: xin@magnet.fsu.edu).

Color versions of one or more of the figures in this paper are available online at http://ieeexplore.ieee.org.

Digital Object Identifier 10.1109/TED.2016.2589272

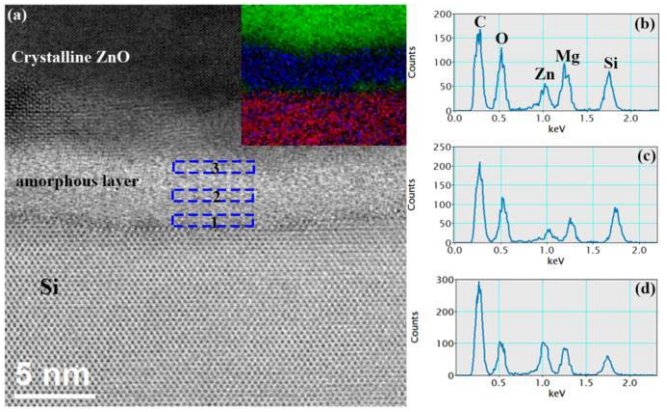

Fig. 1. (a) STEM ABF image of ZnO/MgO/n+-Si. Inset: elemental map (Zn: green; Mg: blue; Si: Red). (b) EDS spectrum of area 1 in (a). (c) EDS spectrum of area 2. (d) EDS spectrum of area 3.

system, respectively. The Si substrates were dipped into piranha solution (H_2SO_4:H_2O_2 = 5:3) and diluted HF alternately for 1 min each for 3 times, rinsed by deionized water in between and after, and finally dried by nitrogen gun before being transferred into an MBE intro-chamber. Mg and Zn sources were provided by two regular Knudsen-cells filled with elemental Mg (6N) and Zn (6N), respectively. O source was provided by an RF plasma source sustained with O_2 (6N) gas. A mass flow controller was used to precisely tune the O_2 flow rate. The MgO layers were grown at 440 °C, with 455 °C Mg cell temperature, 5 standard cubic centimeter per minute (SCCM) O_2 gas flow rate, and 400 W oxygen plasma power for all related samples. The ZnO layers were grown at 400 °C, with 340 °C Zn cell temperature, 5 SCCM O_2 gas flow rate, and 400 W oxygen plasma power for all related samples. Ti (10 nm)/Au (90 nm) square-shaped metal patterns of different areas (50 μm × 50μm, 100 μm × 100μm, 200 μm × 200 μm, 400 μm × 400 μm, and 600 μm × 600 μm) were deposited on ZnO, ZnO/MgO, and MgO by electron beam evaporation after photolithography, followed by standard liftoff process. Al was evaporated also by electron-beam evaporation as back contact onto n^+-Si (100). No high-temperature process was utilized during device fabrication, which can be fully compatible with the back-end CMOS technology [29]. The electrical characteristics of the Au/Ti/ZnO (ZnO/MgO or MgO)/n^+-Si/Al structure were measured by using an Agilent 4155C semiconductor analyzer.

III. Results and Discussion

Fig. 1(a) shows atomic resolution scanning transmission electron microscopy (STEM) annular bright field (ABF) image of as grown ZnO/MgO /n^+-Si structure. It can be observed that there is one amorphous layer of about 4-nm thick between top crystalline ZnO and bottom Si substrate. The elemental map by STEM electron energy loss spectroscopy spectrum imaging is shown in the inset of Fig. 1(a), where Zn shown as green color, Mg as blue color, and Si as red color. The energy dispersive X-ray spectroscopy (EDS) spectra collected from three regions labeled 1 to 3 within the amorphous layer in Fig. 1(a) are shown in Fig. 1(b)–(d), respectively. The amorphous layer is the mixture of ZnO and MgO with more MgO close to Si substrate and more ZnO close to the crystalline ZnO.

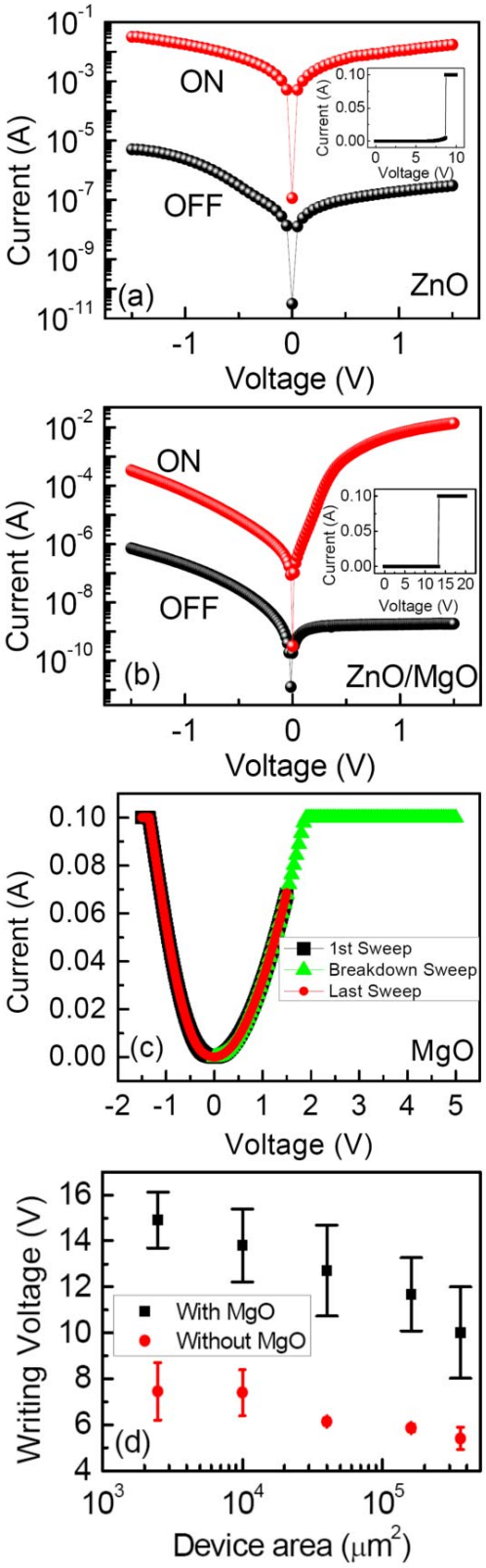

Fig. 2. *I–V* characteristics at current compliances of 100 mA for (a) Au/Ti/ZnO/n^+-Si/Al, (b) Au/Ti/ZnO/MgO/n^+-Si/Al, and (c) Au/Ti/MgO/n^+-Si/Al structures. (d) Writing voltage distribution for WORM devices with different areas using ZnO and ZnO/MgO as active layers.

Fig. 2(a)–(c) show *I–V* characteristics of Au/Ti/ZnO/n^+-Si/Al, Au/Ti/ZnO/MgO/n^+-Si/Al, and Au/Ti/MgO/n^+-Si/Al structures, respectively. First, the applied voltage was swept

from −1.5 to 1.5 V to read the OFF states of WORM, as the black dots shown in Fig. 2(a)–(c). Then, the voltage was swept from 0 to 10 V, 0 to 20 V, and 0 to 5 V to switch the device from OFF to ON states of WORM for ZnO, ZnO/MgO, and MgO structure, respectively, as shown in the inset of Fig. 2(a) and (b) and green triangle in Fig. 2(c). Finally, the applied voltage was swept from −1.5 to 1.5 V again to obtain the current of ON states, as the red dots shown in Fig. 2(a)–(c). During the voltage sweep, the current compliance was set at 100 mA. The resistance ratios of OFF and ON (R-ratio) at a reading voltage of 1 V are about 10^4 and 10^7 for the devices using ZnO and ZnO/MgO as active layers, respectively. For the devices with a MgO layer of only a few nanometers, the resistances are the same before and after writing, as shown in Fig. 2(c), indicating that there is no memory effect. The writing voltage of the devices with MgO layer is higher than that of without MgO layer. Fig. 2(d) shows the distribution of writing voltage of the devices with different areas using ZnO and ZnO/MgO as active layers. The writing voltage of the devices without MgO layer is 5–8 V while it is 10–15 V for the devices with MgO layers. Furthermore, both voltages decrease with the increase of device area, which is similar to the results reported in [30]. This trend may be due to the increase of the edge defect numbers and grain boundaries with the increasing area. After the devices are switched to ON states, they cannot be switched back to OFF states anymore at the current compliance of 100 mA by voltage sweeping from 5 to −5 V for both ZnO and ZnO/MgO devices, indicating WORM properties.

As the current compliance is set at 5 mA, it is observed that the devices using ZnO as an active layer can be completely switched back from OFF to ON if the applied voltage is swept from 5 to −5 V (RS modes), as shown in Fig. 3(a). The prior OFF and ON states for WORM are provided here as black squares and red solid circles, respectively, for comparison. The switching between ON and OFF is reversible, indicating RS properties instead of WORM. The devices using ZnO/MgO as active layer cannot be switched back to OFF state no matter what kind of voltage is applied on the device, as shown in Fig. 3(b).

I–V measurements were performed for devices using ZnO and ZnO/MgO as active layers at other current compliances of 100 μA, 500 μA, 1 mA, 10 mA, and 50 mA. The resistances of OFF and ON states at a reading voltage of 1 V for WORM are written as $R_{W\mathrm{OFF}}$ and $R_{W\mathrm{ON}}$, respectively. The resistances reading at 1 V after the devices go through the voltage sweep of 5 ∼ −5 V and −5 ∼ 5 V were written as $R_{R\mathrm{OFF}}$ and $R_{R\mathrm{ON}}$, respectively. The results are shown in Fig. 4 for devices using (a) ZnO and (b) ZnO/MgO as active layers, respectively. For devices using ZnO as active layer, as shown in Fig. 4(a), the values of $R_{R\mathrm{OFF}}$ and $R_{R\mathrm{ON}}$ are almost the same as those of $R_{W\mathrm{ON}}$ at current compliance of 100 μA, 500 μA, and 1 mA, indicating WORM property only. When the current compliances increase to 5 and 10 mA, the values of $R_{R\mathrm{OFF}}$ are the same as those of $R_{W\mathrm{OFF}}$ while the values of $R_{R\mathrm{ON}}$ are the same as those of $R_{W\mathrm{ON}}$, indicating that devices exhibit RS property instead of WORM property. All the values of $R_{W\mathrm{OFF}}$, $R_{W\mathrm{ON}}$, $R_{R\mathrm{OFF}}$, and $R_{R\mathrm{ON}}$ are different at current compliances of 20, 50, and 100 mA, while $R_{R\mathrm{OFF}}$ and $R_{R\mathrm{ON}}$ are at the same amplitude order of $R_{W\mathrm{OFF}}$, indicating coexistence of WORM and RS. For devices using ZnO/MgO as active layer, as shown in Fig. 4(b), $R_{R\mathrm{OFF}}$ and $R_{R\mathrm{ON}}$ are the same as $R_{W\mathrm{ON}}$ at all current compliances, indicating perfect WORM properties. These results show that a few nanometers layer of MgO can effectively prevent devices from reset.

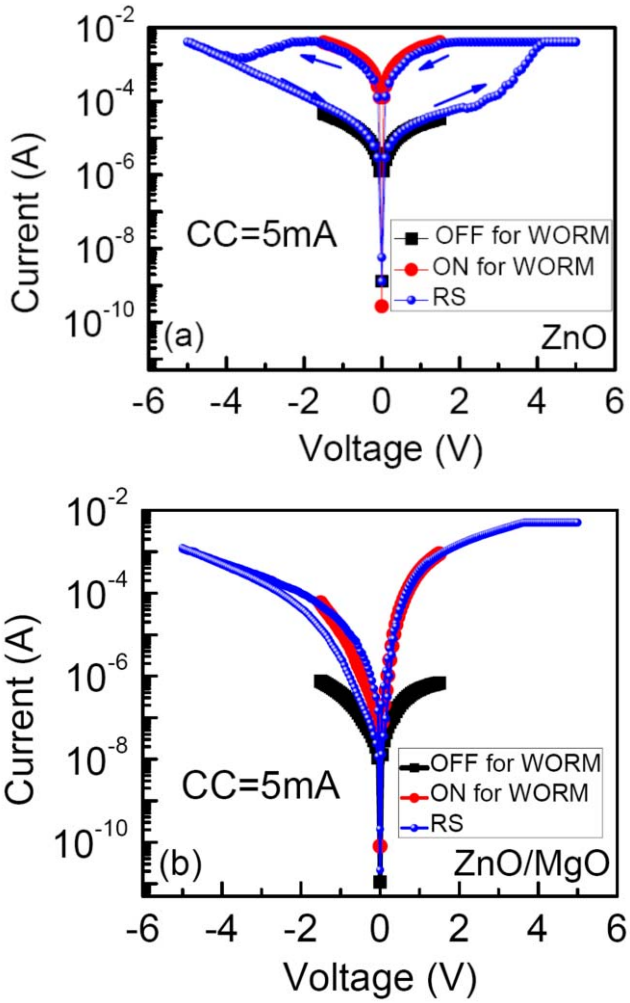

Fig. 3. I–V characteristics at current compliances of 5 mA using (a) ZnO and (b) ZnO/MgO as active layer.

In previous publication [24], it is reported that the conducting filaments consisting of oxygen vacancies are responsible for the switching mechanism from OFF state to ON state. In order to investigate the effect of MgO layer preventing devices from reset, a simple model is proposed based on ZnO and MgO film with a size of 100 μm × 100 μm × 2 nm, respectively. The average drift velocities of oxygen vacancy in ZnO and MgO in this model were calculated according to [31]

$$v \approx \mathrm{fae}^{-\frac{U_A}{k_B T}} \sinh\left(\frac{qEa}{2k_B T}\right)$$

where $f = 10^{13}$ Hz is attempt-to-escape frequency which is usually accepted to be the lattice vibration frequency [32]. $a = 0.52$ nm [33] and 0.42 nm [34] are lattice constants of ZnO (along the c-axis) and MgO. $U_A = 1$ is the migration

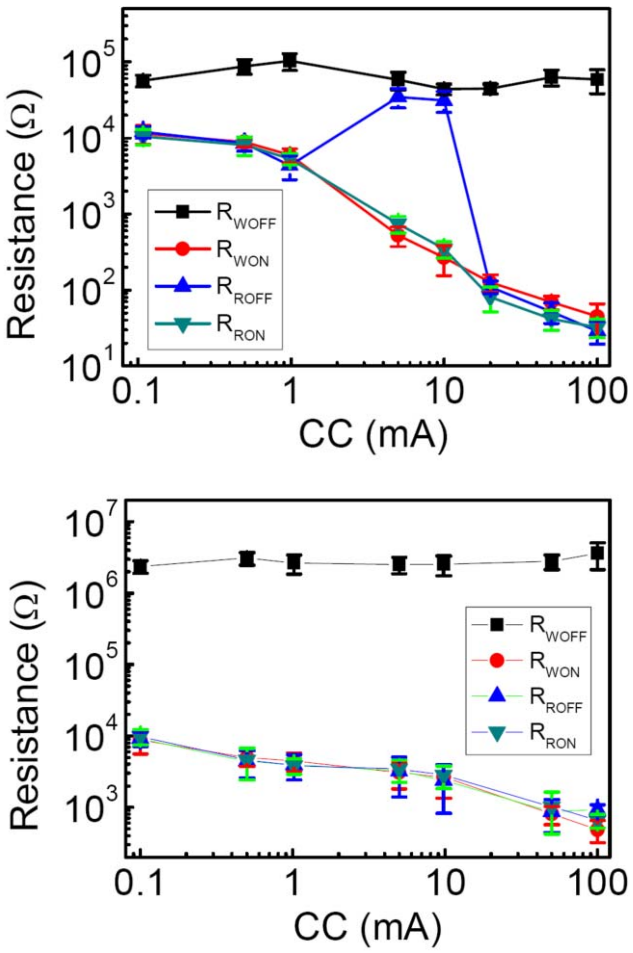

Fig. 4. Resistance of OFF and ON states at a different current compliance measured at WORM and RS modes for devices using (a) ZnO and (b) ZnO/MgO as active layer.

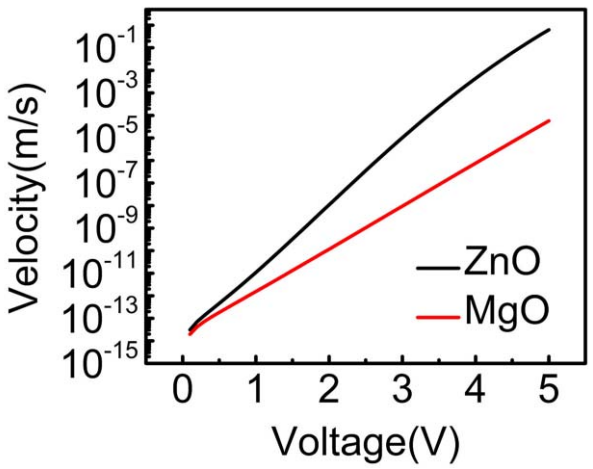

Fig. 5. Estimated drift velocity of oxygen vacancy in ZnO and MgO versus the absolute value of applied voltages.

energy of oxygen vacancy. E is the local electric field for the oxygen vacancy drift determined by the applied bias and the thickness of ZnO or MgO. k_B, T, and q are Boltzmann constant, local temperature, and charge of oxygen vacancy, respectively. Because of Joule heating, the local temperature can rise to a steady-state value in nanoseconds under an applied bias. The local temperature is given by [35]

$$T = T_0 + \frac{V^2}{R} R_{\text{th}}$$

where $T_0 = 297$ K, $R_{\text{th}} = 10$ K/W is equivalent thermal resistance, V is bias, R is resistance of ZnO and MgO thin film calculated from the data in Fig. 2(a) and (c), which are about 1.2 and 46 Ω, respectively. It shall be noted that although the formula is for crystalline materials, it is still suitable to compare the difference between ZnO and MgO approximately because the impact of lattice constants on the average drift velocity is much weaker than that of other factors. The calculated results shown in Fig. 5 indicate that the drift velocity of oxygen vacancy in ZnO is at least ten times larger than that in MgO under given voltage from 1 to 5 V. Therefore, the probability of recombination between O^{2-} and oxygen vacancy is much lower in MgO than that in ZnO. In other words, the oxygen vacancy in MgO is much more stable than that in ZnO. Meanwhile, it is obvious that the difference of average drift velocity of oxygen vacancy in ZnO and MgO becomes larger with the increase of bias because the resistance of ZnO is lower than that of MgO. Thus, the temperature rises faster with the increase of voltage in ZnO, leading to the fact that the velocity of oxygen vacancy in ZnO increases faster than that in MgO. O^{2-} ions accumulate on the interface of ZnO and MgO during the transport when there is a 2-nm MgO layer. These negatively charged O^{2-} ions form a local electric field, which weakens the effective electric field in the ZnO layer and enhances the effective electric field in MgO. Furthermore, the drift velocity increases much quicker with the increase of applied voltage in ZnO than that in MgO. Therefore, higher voltage is needed to obtain the same drift velocity of oxygen vacancy forming the conducting filaments in devices using ZnO/MgO, which explains the higher writing voltage of devices using ZnO/MgO. As the devices were fabricated with ZnO only, the voltage of −5 V is enough to switch back the device to OFF states immediately because of the breaking of conducting filaments at high oxygen vacancy drift velocity. While there is an embedded MgO layer of a few nanometers, the devices cannot be switched back to OFF states at once because the much lower drift velocity of oxygen vacancy in MgO and accumulation of negatively charged O^{2-} ions at the interface between ZnO and MgO prevent the conducting filaments composed of oxygen vacancies from breaking.

IV. Conclusion

WORM devices were fabricated using Au/Ti/ZnO/n^+-Si/Al and Au/Ti/ZnO/MgO/n^+-Si/Al structures. The I–V characteristics show that the devices fabricated with ZnO layer have RS, WORM, or RS/WORM coexisting properties at different current compliances, while devices using ZnO/MgO as active layer show WORM only at all current compliances. The huge difference of oxygen vacancy velocity in ZnO and MgO plays a major role in the effect of MgO preventing devices from reset.

REFERENCES

[1] R. Waser, R. Dittmann, G. Staikov, and K. Szot, "Redox-based resistive switching memories—Nanoionic mechanisms, prospects, and challenges," *Adv. Mater.*, vol. 21, nos. 25–26, pp. 2632–2663, Jul. 2009.

[2] R. Waser and M. Aono, "Nanoionics-based resistive switching memories," *Nature Mater.*, vol. 6, no. 11, pp. 833–840, Nov. 2007.

[3] A. Sawa, "Resistive switching in transition metal oxides," *Mater. Today*, vol. 11, no. 6, pp. 28–36, Jun. 2008.

[4] S. H. Jo and W. Lu, "CMOS compatible nanoscale nonvolatile resistance switching memory," *Nano Lett.*, vol. 8, no. 2, pp. 392–397, Jan. 2008.

[5] S. H. Jo, K.-H. Kim, and W. Lu, "Programmable resistance switching in nanoscale two-terminal devices," *Nano Lett.*, vol. 9, no. 1, pp. 496–500, Dec. 2008.

[6] S. Möller, C. Perlov, W. Jackson, C. Taussig, and S. R. Forrest, "A polymer/semiconductor write-once read-many-times memory," *Nature*, vol. 426, no. 6963, pp. 166–169, Nov. 2003.

[7] H. Li *et al.*, "Two different memory characteristics controlled by the film thickness of polymethacrylate containing pendant azobenzothiazole," *J. Phys. Chem. C*, vol. 114, no. 13, pp. 6117–6122, Mar. 2010.

[8] J. Lin and D. Ma, "The morphology control of pentacene for write-once-read-many-times memory devices," *J. Appl. Phys.*, vol. 103, no. 2, pp. 024507-1–024507-4, Jan. 2008.

[9] M. A. Mamo, W. S. Machado, W. A. L. van Otterlo, N. J. Coville, and I. A. Hümmelgen, "Simple write-once-read-many-times memory device based on a carbon sphere-poly(vinylphenol) composite," *Org. Electron.*, vol. 11, no. 11, pp. 1858–1863, Nov. 2010.

[10] M. W. Cho, A. Setiawan, H. J. Ko, S. K. Hong, and T. Yao, "ZnO epitaxial layers grown on c-sapphire substrate with MgO buffer by plasma-assisted molecular beam epitaxy (P-MBE)," *Semicond. Sci. Technol.*, vol. 20, no. 4, pp. S13–S21, Mar. 2005.

[11] G. Chen, C. Song, C. Chen, S. Gao, F. Zeng, and F. Pan, "Resistive switching and magnetic modulation in cobalt-doped ZnO," *Adv. Mater.*, vol. 24, no. 26, pp. 3515–3520, Jul. 2012.

[12] J.-J. Ke, Z.-J. Liu, C.-F. Kang, S.-J. Lin, and J.-H. He, "Surface effect on resistive switching behaviors of ZnO," *Appl. Phys. Lett.*, vol. 99, no. 19, pp. 192106-1–192106-3, Nov. 2011.

[13] Q. Mao, Z. Ji, and J. Xi, "Realization of forming-free ZnO-based resistive switching memory by controlling film thickness," *J. Phys. D, Appl. Phys.*, vol. 43, no. 39, pp. 395104-1–395104-5, Oct. 2010.

[14] S. Lee, H. Kim, J. Park, and K. Yong, "Coexistence of unipolar and bipolar resistive switching characteristics in ZnO thin films," *J. Appl. Phys.*, vol. 108, no. 7, pp. 076101-1–076101-3, Oct. 2010.

[15] J. Qi, J. Ren, M. Olmedo, N. Zhan, and J. Liu, "Unipolar resistive switching in Au/Cr/$Mg_{0.84}Zn_{0.16}O_{2-\delta}$ /p^+-Si," *Appl. Phys. A*, vol. 107, no. 4, pp. 891–897, Jun. 2012.

[16] Y. C. Yang, F. Pan, Q. Liu, M. Liu, and F. Zeng, "Fully room-temperature-fabricated nonvolatile resistive memory for ultrafast and high-density memory application," *Nano Lett.*, vol. 9, no. 4, pp. 1636–1643, Feb. 2009.

[17] K. Nagashima *et al.*, "Resistive switching multistate nonvolatile memory effects in a single cobalt oxide nanowire," *Nano Lett.*, vol. 10, no. 4, pp. 1359–1363, Apr. 2010.

[18] Y. Yang *et al.*, "Nonvolatile resistive switching in single crystalline ZnO nanowires," *Nanoscale*, vol. 3, no. 4, pp. 1917–1921, 2011.

[19] J. Qi, J. Huang, D. Paul, J. Ren, S. Chu, and J. Liu, "Current self-complianced and self-rectifying resistive switching in Ag-electroded single Na-doped ZnO nanowires," *Nanoscale*, vol. 5, no. 7, pp. 2651–2654, 2013.

[20] J. Qi *et al.*, "Resistive switching in single epitaxial ZnO nanoislands," *ACS Nano*, vol. 6, no. 2, pp. 1051–1058, Feb. 2012.

[21] I.-C. Yao, D.-Y. Lee, T.-Y. Tseng, and P. Lin, "Fabrication and resistive switching characteristics of high compact Ga-doped ZnO nanorod thin film devices," *Nanotechnology*, vol. 23, no. 14, pp. 145201-1–145201-8, Apr. 2012.

[22] W.-Y. Chang, C.-A. Lin, J.-H. He, and T.-B. Wu, "Resistive switching behaviors of ZnO nanorod layers," *Appl. Phys. Lett.*, vol. 96, no. 24, pp. 242109-1–242109-3, Jun. 2010.

[23] J. Qi, M. Olmedo, J.-G. Zheng, and J. Liu, "Multimode resistive switching in single ZnO nanoisland system," *Sci. Rep.-UK*, vol. 3, pp. 2405-1–2405-6, Aug. 2013.

[24] J. Qi, Q. Zhang, J. Huang, J. Ren, M. Olmedo, and J. Liu, "Write-once–read-many-times memory based on ZnO on p-Si for long-time archival storage," *IEEE Electr. Device Lett.*, vol. 32, no. 10, pp. 1445–1447, Oct. 2011.

[25] J. Qi, Q. Zhang, and J. Liu, "The effect of top contact on ZnO write-once–read-many-times memory," *Phys. Status Solidi Rapid Res. Lett.*, vol. 6, no. 12, pp. 478–480, Dec. 2012.

[26] H. Kato, K. Miyamoto, M. Sano, and T. Yao, "Polarity control of ZnO on sapphire by varying the MgO buffer layer thickness," *Appl. Phys. Lett.*, vol. 84, no. 22, pp. 4562–4564, May 2004.

[27] P. Bhattacharya, R. R. Das, and R. S. Katiyar, "Fabrication of stable wide-band-gap ZnO/MgO multilayer thin films," *Appl. Phys. Lett.*, vol. 83, no. 10, pp. 2010–2012, Sep. 2003.

[28] A. Shih *et al.*, "Highly stable resistive switching on monocrystalline ZnO," *Nanotechnology*, vol. 21, no. 12, pp. 125201-1–125201-6, Mar. 2010.

[29] R. Huang *et al.*, "Resistive switching of silicon-rich-oxide featuring high compatibility with CMOS technology for 3D stackable and embedded applications," *Appl. Phys. A*, vol. 102, no. 4, pp. 927–931, Mar. 2011.

[30] B. Singh, B. R. Mehta, D. Varandani, A. V. Savu, and J. Brugger, "CAFM investigations of filamentary conduction in Cu_2O ReRAM devices fabricated using stencil lithography technique," *Nanotechnology*, vol. 23, no. 49, pp. 495707-1–495707-10, Nov. 2012.

[31] D. B. Strukov and R. S. Williams, "Exponential ionic drift: Fast switching and low volatility of thin-film memristors," *Appl. Phys. A*, vol. 94, no. 3, pp. 515–519, Mar. 2009.

[32] S. A. Studenikin, N. Golego, and M. Cocivera, "Optical and electrical properties of undoped ZnO films grown by spray pyrolysis of zinc nitrate solution," *J. Appl. Phys.*, vol. 83, no. 4, pp. 2104–2111, Feb. 1998.

[33] Ü. Özgür *et al.*, "A comprehensive review of ZnO materials and devices," *J. Appl. Phys.*, vol. 98, no. 4, pp. 041301-1–041301-103, Aug. 2005.

[34] B. H. Park *et al.*, "Effects of very thin strain layers on dielectric properties of epitaxial $Ba_{0.6}Sr_{0.4}TiO_3$ films," *Appl. Phys. Lett.*, vol. 78, no. 4, pp. 533–535, Jan. 2001.

[35] S. Yu and H.-S. P. Wong, "A phenomenological model for the reset mechanism of metal oxide RRAM," *IEEE Electron Device Lett.*, vol. 31, no. 12, pp. 1455–1457, Dec. 2010.

Bosen Zhang is currently pursuing the B.S degree with the Department of Physics, School of Physical Science and Technology, Lanzhou University, Lanzhou, China.

He has been an Undergraduate Research Assistant with the Key Laboratory for Magnetism and Magnetic Materials of MOE, Lanzhou University, since 2014.

Cong Hu is currently pursuing the M.S. degree in condensed matter physics, School of Physical Science and Technology, Lanzhou University, Lanzhou, China.

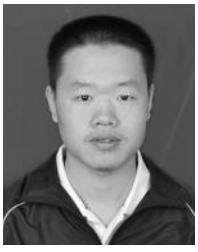

Tianshuang Ren is currently pursuing the B.S. degree with the Department of Physics, School of Physical Science and Technology, Lanzhou University, Lanzhou, China.

He has been an Undergraduate Research Assistant with the Key Laboratory for Magnetism and Magnetic Materials of MOE, Lanzhou University, since 2014.

Bo Wang is currently pursuing the B.S degree with the Department of Physics, School of Physical Science and Technology, Lanzhou University, Lanzhou, China.

He has been an Undergraduate Research Assistant with the Key Laboratory for Magnetism and Magnetic Materials of MOE, Lanzhou University, since 2014.

Jing Qi was born in 1974. She received the Ph.D. degree in condensed matter physics from Lanzhou University, Lanzhou, China, in 2006.

She is currently a Professor with Lanzhou University, Lanzhou, China. Her research interests include diluted magnetic semiconductor materials, novel memory devices, and semiconductor nanowires.

Qing Zhang received the M.S. degree in electrical engineering from the University of California at Riverside, Riverside, CA, USA, in 2011.

Jian-Guo Zheng received the B.S., M.S., and Ph.D. degrees from Nanjing University, Nanjing, China, in 1983, 1989, 1992, respectively, all in solid state physics.

He is currently the Director of Operations with the Laboratory for Electron and Xray Instrumentation, and the Project Scientist (VII), California Institute for Telecommunication and Information Technology (Irvine division), University of California at Irvine, Irvine, CA, USA. His current research interests include electron microscopy, materials physics, and research facility management.

Yan Xin was born in 1966. She received the Ph.D. degree from the Materials Science and Metallurgy Department, University of Cambridge, Cambridge, U.K.

She is currently an Associate Scientist with the National High Magnetic Field Laboratory, Florida State University, Tallahassee, FA, USA. Her current research interests include the materials research by transmission electron microscopy.

Jianlin Liu (M'02) received the Ph.D. degree in electrical engineering from the University of California at Los Angeles, CA, USA in 2003.

He joined the Department of Electrical Engineering, University of California at Riverside, Riverside, USA, in 2003, where he is currently a Full Professor.